designs

MDPI

Article

Experimental Fitting of Efficiency Hill Chart for Kaplan Hydraulic Turbine

Roberto Capata [1], Alfonso Calabria [2], Gian Marco Baralis [3] and Giuseppe Piras [1,*]

[1] Department of Astronautical, Electrical and Energy Engineering (DIAEE), Sapienza University of Rome, 00184 Rome, Italy; roberto.capata@uniroma1.it
[2] Faculty of Engineering, University eCampus, 10-22060 Novedrate, Italy; alfonso.calabria@uniecampus.it
[3] BGM Co., 12021 Acceglio, Italy; bgmgmb@gmail.com
* Correspondence: giuseppe.piras@uniroma1.it

Abstract: The development of hydroelectric technology and much of the "knowledge" on hydraulic phenomena derive from scale modeling and "bench" tests to improve machinery efficiency. The result of these experimental tests is mapping the so-called "hill chart", representing the "DNA" of a turbine model. Identifying the efficiency values as a function of the specific parameters of the flow and energy coefficient (which both identify the operating point) allows us to represent the complete behavior of a turbine in hydraulic similarity with the original model developed in the laboratory. The present work carries out a "reverse engineering" operation that leads to the definition of "an innovative research model" that is relatively simple to use in every field. Thus, from the experimental survey of the degree of efficiency of several prototypes of machines deriving from the same starting model, the hill chart of the hydraulic profile used is reconstructed. The "mapping" of all the characteristic quantities of the machine, together with the physical parameters of the regulating organs of a four-blade Kaplan turbine model, also made it possible to complete the process, allowing to identify not only the iso-efficiency regions but also the curves relating to the trend of the angle of the impeller blades, the specific opening of the distributor, and the identification of critical areas of cavitation. The development of the hill chart was made possible by investigating the behavior of 33 actual prototypes and 46 characteristic curves derived from the same reference model based on practical experiments for finding the optimal blade distributor "setup curve". To complete this, theoretical characteristic curves of "not physically realized" prototypes were also mapped, allowing us to complete the regions comprising the diagram. The study of the unified hill charts found in previous documentation of the most famous manufacturers was of great help. Finally, the validation of the "proposed procedure" was obtained through the experimental survey of the actual efficiency of the new prototype based on the theoretical values defined in the design phase on the chart obtained with the method described.

Keywords: hydraulic turbine designs; experimental chart evaluation; reverse engineering method; innovative procedure; hill chart assembling; component optimization

Citation: Capata, R.; Calabria, A.; Baralis, G.M.; Piras, G. Experimental Fitting of Efficiency Hill Chart for Kaplan Hydraulic Turbine. *Designs* **2024**, *8*, 80. https://doi.org/10.3390/designs8040080

Academic Editors: José António Correia, Shuaishuai Wang and Yihan Xing

Received: 23 April 2024
Revised: 26 June 2024
Accepted: 8 August 2024
Published: 13 August 2024

1. Introduction: The Characteristic Curves of Hydraulic Turbines

The "characteristic curves", or more simply the "characteristics", are the graphic representations of one or more hydraulic or mechanical parameters of the hydraulic machine [1–4]. Tracing these graphs constitutes the most comprehensive and summary method to highlight the design properties and verify their compatibility with the application and its theoretical behavior. The most significant graph is the efficiency map of the machine as a function of the degree of partialization. The "partialization" does not represent the degree of opening [in%] of the distributor but rather the flow rate that can be effectively processed by the turbine defined in [m^3/s]. This graph is created for each machine once the geometry and diameter D with the parameters such as rotational speed "n" (constant)

and net operative head H_n (considered constant) within all operating ranges have been established. Usually, this graph contains the curve that represents the power delivered (to the turbine axis) as a function of the flow rates processed [5–7]. This graphic representation shows the performance of the defined and studied machine.

The curves may show indicative trends (especially at low-angle distributor openings) and highlight the nominal values. Concerning the standards defined by the IEC 60041 [5], the efficiency values refer to an operating "Net Head" (H_n). This value is known to be identified in the nominal flow rate ($\dot{Q}$ n) condition (excluding overflow conditions). The standard indicates that, if the actual conditions differ by no more than ±10% (refers to the head), it is necessary to use average values and normalize the values obtained with the similarity. If the test conditions significantly differ from the tolerance reported by the standard, a correction must be made. To overcome this situation, it is possible, after defining a curve representing the head as a function of flow rate [5,6], to determine an efficiency curve as a function of a variable head [7] (a condition that always tends to occur in the operational conditions). However, it is difficult to determine "a priori" for this load variation, and often, efficiency curves are presented for different net heads. Figures 1 and 2 show two operating curves of an actual prototype under various operating conditions. Based on this information, the similarity can be applied, considering the efficiency values "very close" to the exact operating conditions. In addition to these data, which represent the "nominal" behavior of the turbine, some manufacturers can provide general information about the reference model (Table 1, Figures 1 and 2).

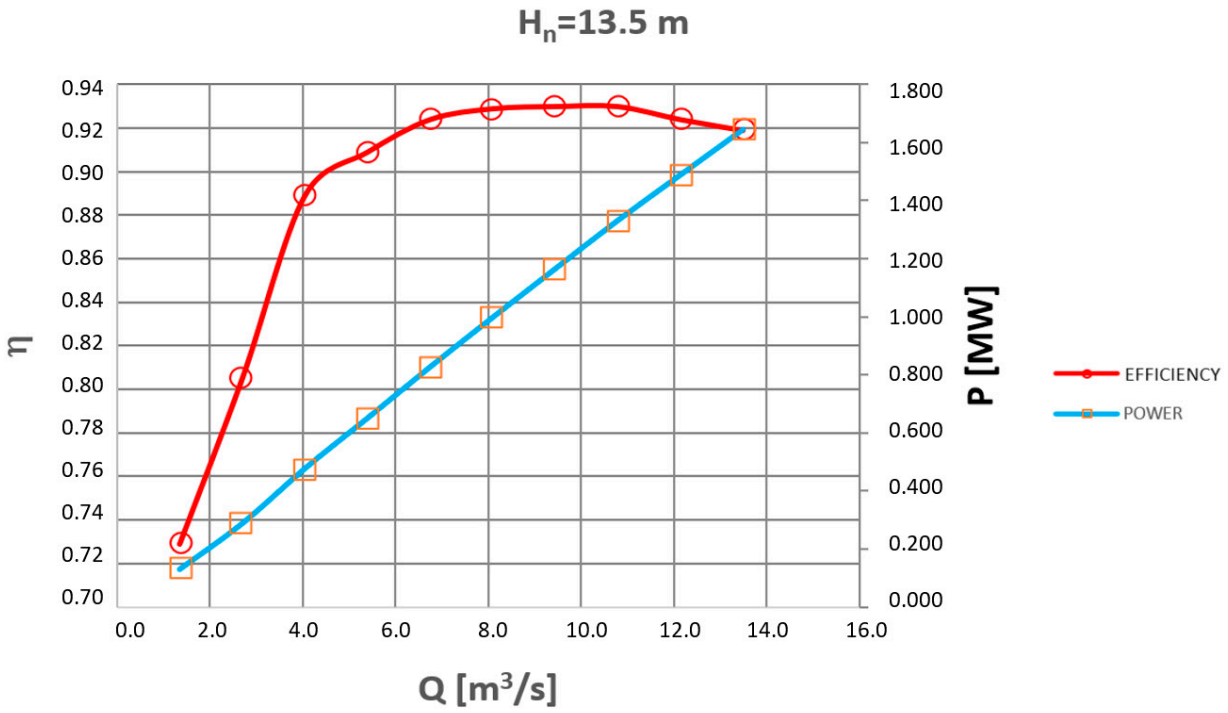

Figure 1. Operational map of real model H_n =13.5 m.

Table 1. Example of turbine operating parameters.

Model Type	Turbine Characteristics		
Optimal flow coefficient	ϕ_{opt}	0.20	[-]
Optimal load coefficient	ψ_{opt}	0.36	[-]
Model optimum efficiency	η_{opt}	0.915	[-]
Specific speed	Ns	554	[-]
Flow coefficient max at ψ_{opt}	ϕ_{opt}	0.34	[-]

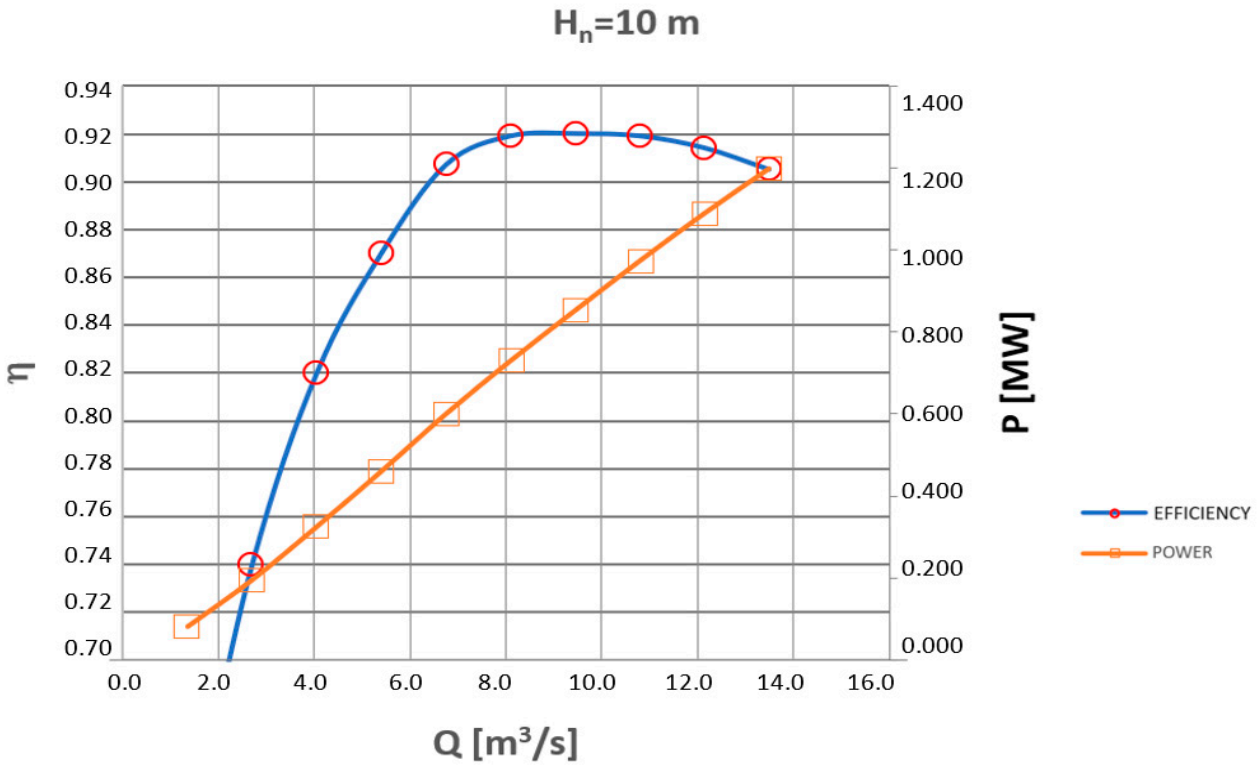

Figure 2. Operational map of real model H_n = 10 m.

2. The Operational Parameters

The "characteristic curve" defines the behavior of the turbine at the rated operating conditions [1–3,8]. This map is a summary of the operating conditions without providing information on the specific parameters of the machine. The values that identify the operating characteristics of the turbine, in this case a Kaplan reaction turbine with double regulation, are different. These quantities can be summarized as follows:

1. Specific speed $N_s = \frac{3.65 \cdot n \cdot \sqrt[2]{Q}}{H^{0.75}}$;
2. Flow coefficient $\varphi = \frac{Q}{\frac{\pi^2}{4} \cdot n^2 \cdot D^3}$;
3. Load coefficient $\psi = \frac{H}{\frac{\pi^2}{2g} \cdot n^2 \cdot D^2}$.

Then, from the law of proportionality,

$$\frac{H'}{H} = \left(\frac{n'}{n}\right)^2 = \left(\frac{Q'}{Q}\right)^2$$

The specific values of the considered reference model are as follows:

- Model-specific flow rate: $\dot{Q}_1' = \frac{Q}{D^2 \sqrt[2]{H}}$;
- Model-specific speed: $n_1' = \frac{nD}{\sqrt[2]{H}}$.

The above equations are replaced by the coefficients φ and ψ. With these parameters, it is possible to know the specific behavior of the machine for the two values of the net head (Table 2). "Characteristic curves" refer to the machine prototype realized with "real" dimensions.

The prototype is studied based on laboratory information about the reference model considering the "scale effects". The methodology of the calculation of the scale effects is regulated by the IEC 995 [9] and IEC 193 [10] standards, where the dimensions and the calculation methodology for the conversion of hydraulic performance data from the model to the prototype with hydraulically similar operating conditions are defined [11–13]. In this

case, applying the scale-up criteria, the prototype shows an increase equal to $\Delta\eta = 1.87\%$ compared to the values of the reference model with a diameter $D_m = 300$ mm.

Table 2. Operating parameters of the turbine for different heads.

H_n = 13.5 m					H_n = 10 m				
Q [m³/s]	**H_n [m]**	**ψ [-]**	**φ [-]**	**η [%]**	**Q [m³/s]**	**H_n [m]**	**ψ [-]**	**φ [-]**	**η [%]**
1.35	13.5	0.387	0.029	72.9	1.35	10	0.287	0.029	62
2.7	13.5	0.387	0.058	80.5	2.7	10	0.287	0.058	74
4.05	13.5	0.387	0.087	88.9	4.05	10	0.287	0.088	82
5.4	13.5	0.387	0.116	90.9	5.4	10	0.287	0.117	87
6.75	13.5	0.387	0.146	92.4	6.75	10	0.287	0.146	90.7
8.1	13.5	0.387	0.175	92.9	8.1	10	0.287	0.175	91.9
9.45	13.5	0.387	0.204	93	9.45	10	0.287	0.204	92
10.8	13.5	0.387	0.233	93	10.8	10	0.287	0.234	91.9
12.15	13.5	0.387	0.262	92.4	12.15	10	0.287	0.263	91.4
13.5	13.5	0.387	0.292	91.9	13.5	10	0.287	0.292	90.5

The small size of the model tested in the laboratory penalizes the efficiency due to the consequent difference in friction losses. Experience has shown that the numbers of Froude, Reynolds, and Weber mainly influence the scale effect. The IEC-995 standard defines the application criteria for reaction turbines, currently excluding action turbines (Pelton) as: "... since these effects have not yet been sufficiently analyzed and there is no theoretical justification, it is impossible to indicate a tried and tested calculation procedure". The characteristic scale models according to IEC 193 are shown in Table 3 and Figure 3.

Table 3. Feature scale models according to IEC 193.

Parameter	**Turbomachinery**			
	Radial (Francis)	**Diagonal (Mixed Flow)**	**Axial (Kaplan, Bulb)**	**Impulse (Pelton)**
Reynolds number Re	4×10^6	4×10^6	4×10^6	2×10^6
Specific hydraulic energy E [J/kg]	100	50	30	500
Reference diameter D [m]	0.25	0.3	0.3	-----
Bucket width [m]	-----	-----	-----	0.08

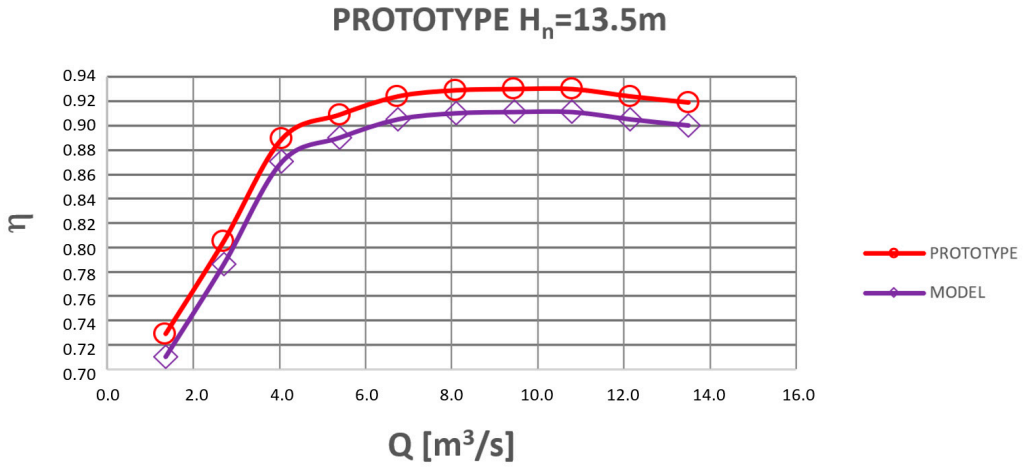

Figure 3. Comparison between model and prototype.

3. The Prototype Tests

The testing phase of a hydraulic turbine allows for the analysis of the machine's actual behavior and the determination of its efficiency [13–15]. The IEC 60041 standard defines this phase, and the results must be analyzed according to the "deviation" from the nominal value of the "considered head". Table 4 shows the results obtained on a prototype of a Kaplan turbine with the main characteristics: D = 1500 mm; n = 333 rpm.

Table 4. Operational data compared with the model.

Runner [%]	Distributor [%]	$\dot{Q}$ [m³/s]	H_n [m]	P [kW]	ψ [-]	φ [-]	$\eta_{prototype}$ [%]	η_{model} [%]
5.5	45	2.86	11.35	260	0.326	0.062	79.6	77.8
8.7	47	3.08	11.19	285	0.321	0.067	81.3	79.4
11	48	3.23	11.05	310	0.317	0.070	84.4	82.5
20	50	4.38	10.87	470	0.312	0.095	88.4	86.6
27	58	5.4	10.71	590	0.307	0.117	90.4	88.5
35	65	6.62	10.52	725	0.302	0.143	91.2	89.3
40	67	7.04	10.42	780	0.299	0.152	92.2	90.4
50	75	8.7	10.19	955	0.292	0.188	92.7	90.8
56	80	9.65	10.03	1050	0.288	0.209	93.0	91.1
65	82	10.7	9.83	1150	0.282	0.232	93.1	91.3
72	85	11.8	9.62	1240	0.276	0.255	92.5	90.6
78	87	12.5	9.44	1290	0.271	0.270	91.9	90.0
80	90	13.3	9.39	1340	0.269	0.288	90.8	89.0
90	97	14.3	9	1410	0.258	0.309	90.3	88.4

Determination of Efficiency Contour Map

Once the operating points have been determined, these values are reported on the diagram, "centering" them (see Figure 4). With the same criterion, the two "strings", referring to the working points corresponding to the different net head conditions, i.e., Hn = 13.5 and 10 m, are inserted (in the diagram in Figure 5). Analogously, the efficiency values in working conditions are inserted (Figure 6). In the map in Figure 6, it is possible to see a good uniformity of the iso-efficiency points' distribution concerning the theoretical conditions of the characteristic diagrams compared with the results of the tests carried out during the test conditions (Figure 7).

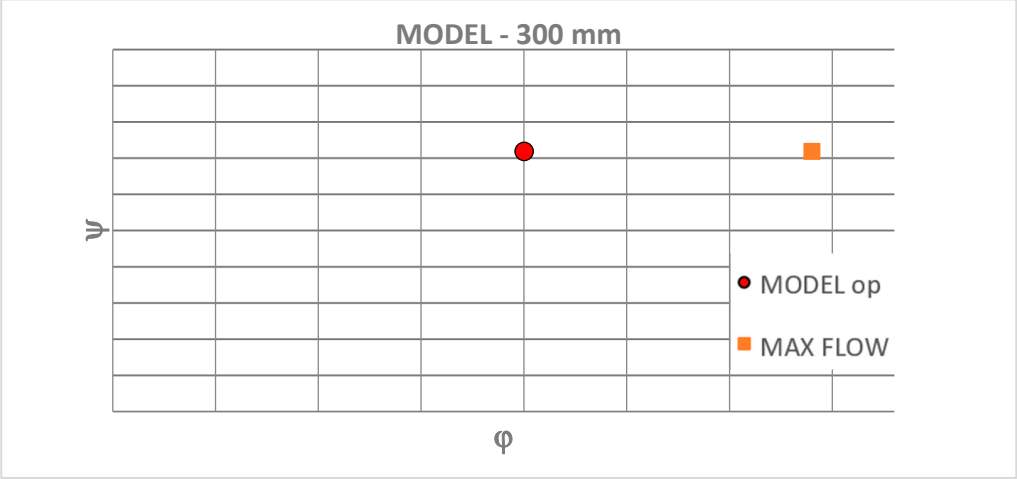

Figure 4. Centering of model nominal values.

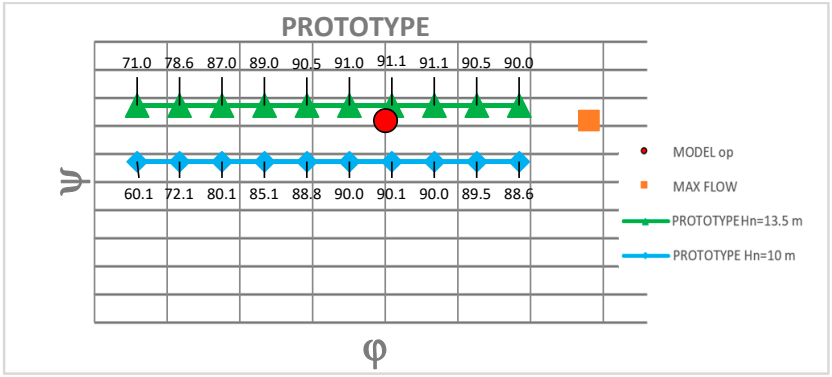

Figure 5. Operating data at different heads.

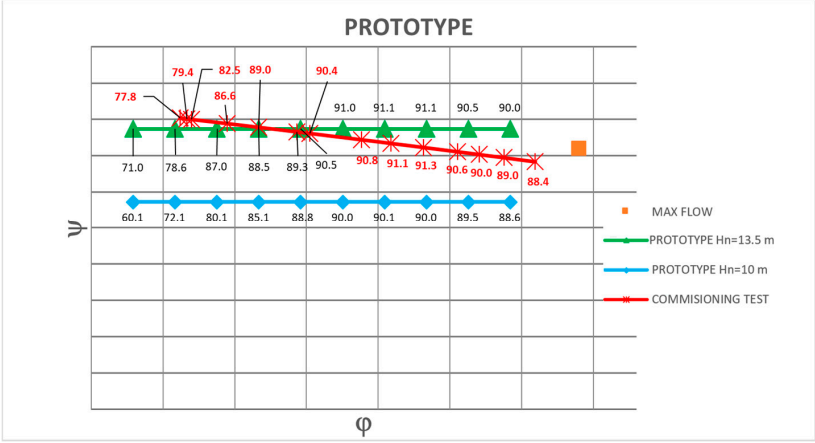

Figure 6. Comparison in actual operative conditions.

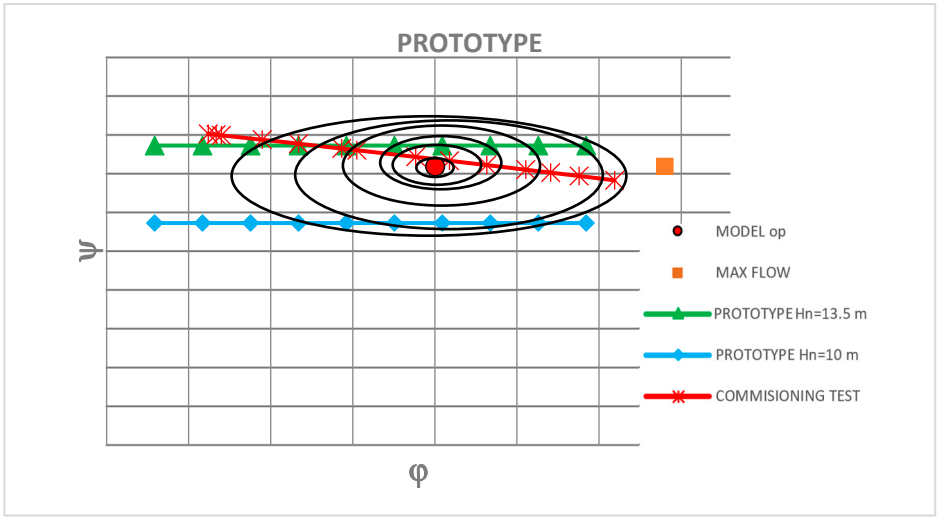

Figure 7. Efficiency contours for considered turbomachinery.

In addition, it can be seen, preliminarily on the prototype made, that the operating characteristics curves in the two different operating conditions are relatively "closed" to the optimal centering value of the reference model. Operational tests were carried out on 33 Kaplan turbine machines. Subsequently, 46 solutions were analyzed since some plants' characteristic curves relating to different proposed heads were collected. Of these 46 solutions, 18 were "theoretical" machines still under construction. The data used in this case were limited to characteristic curves (Q-η) defined by the manufacturer and the distinctive

dimensions and data of the turbine (diameter—number of revolutions—head—flow rate). According to the test results, the remaining ones were actual prototypes in operation for which it was possible to deepen this study (Table 5).

Table 5. Test results.

Plant	Solution	D [mm]	n [rpm]	H [m]	Q [m^3/s]	φ [-]	ψ [-]
1	1	1500	333	333	11.05	0.317	0.292
2	2	950	300	300	4.6	0.405	0.284
3	3	1500	250	250	6.7	0.341	0.317
4	4	700	750	750	11.9	0.309	0.227
5	5	900	428	428	6.9	0.333	0.281
	6	975	375	375	6.9	0.369	0.252
	7	850	428	428	6.9	0.373	0.278
6	8	680	500	500	6.3	0.390	0.309
	9	700	500	500	6.3	0.368	0.284
7	10	1150	375	375	9.7	0.373	0.298
8	11	3500	75	75	3.7	0.384	0.302
9	12	1400	175	175	3.4	0.405	0.304
10	13	800	600	600	12.2	0.379	0.237
11	14	1800	231	231	7.5	0.310	0.271
12	15	1000	500	500	10.8	0.309	0.292
13	16	1450	250	250	6.2	0.338	0.319
14	17	1150	375	375	7.7	0.296	0.277
15	18	1600	250	250	6.6	0.295	0.285
16	19	1900	200	200	6.15	0.305	0.319
17	20	2100	187	187	5.9	0.274	0.329
18	21	2560	167	167	7	0.274	0.295
19	22	2950	136	136	7.8	0.347	0.258
	23	2950	136	136	7.7	0.342	0.258
	24	2950	136	136	9.2	0.409	0.258
	25	2950	136	136	7.4	0.329	0.258
	26	2950	136	136	7.3	0.325	0.258
	27	2950	136	136	9.1	0.405	0.258
	28	2600	200	220	17.5	0.383	0.233
20	29	950	375	375	6	0.338	0.310
21	30	740	375	375	4.25	0.395	0.280
22	31	920	333	333	4.6	0.351	0.281
23	32	3500	75	82	4.2	0.365	0.277
24	33	1250	428	428	14.1	0.353	0.291
	34	1250	428	428	15	0.375	0.291
	35	1250	428	428	16.12	0.403	0.291
25	36	540	600	600	5.5	0.375	0.257
	37	540	600	600	5.5	0.375	0.257
26	38	743	300	300	2.65	0.382	0.267
27	39	2747	187.5	187.5	12.5	0.337	0.288
28	40	1350	300	300	7.5	0.327	0.297
	41	1550	250	250	7.5	0.357	0.235
29	42	2550	120	140	5.9	0.331	0.241
30	43	670	500	500	5.3	0.338	0.323
31	44	550	750	750	9	0.379	0.292
32	45	850	500	500	10.3	0.408	0.277
33	46	5000	100	100	10.3	0.295	0.324

Once the various data were collected, these values were entered in the diagram (Figure 8) by constructing the working points of the machines considered the maximum project opening ($\dot{Q}$ = 100%).

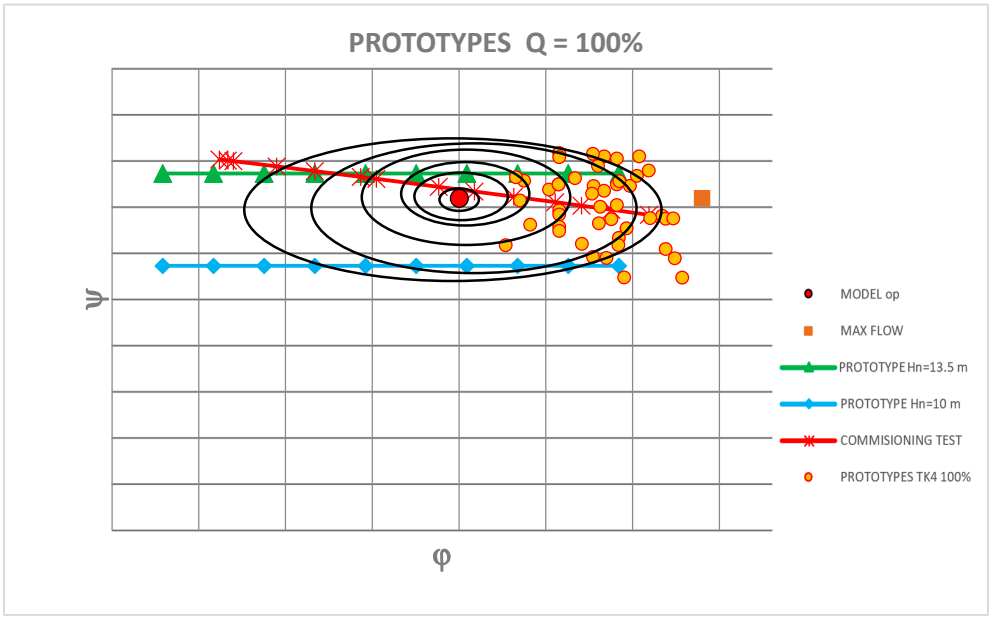

Figure 8. Working points of the machines.

Then, the operating points relating to the reduced flow rate ($\dot{Q}$ = 80%, Figure 9) were checked for the same machines. This value (80 ÷ 85%) corresponds to the "centering" value usually set in a Kaplan turbine's design phase.

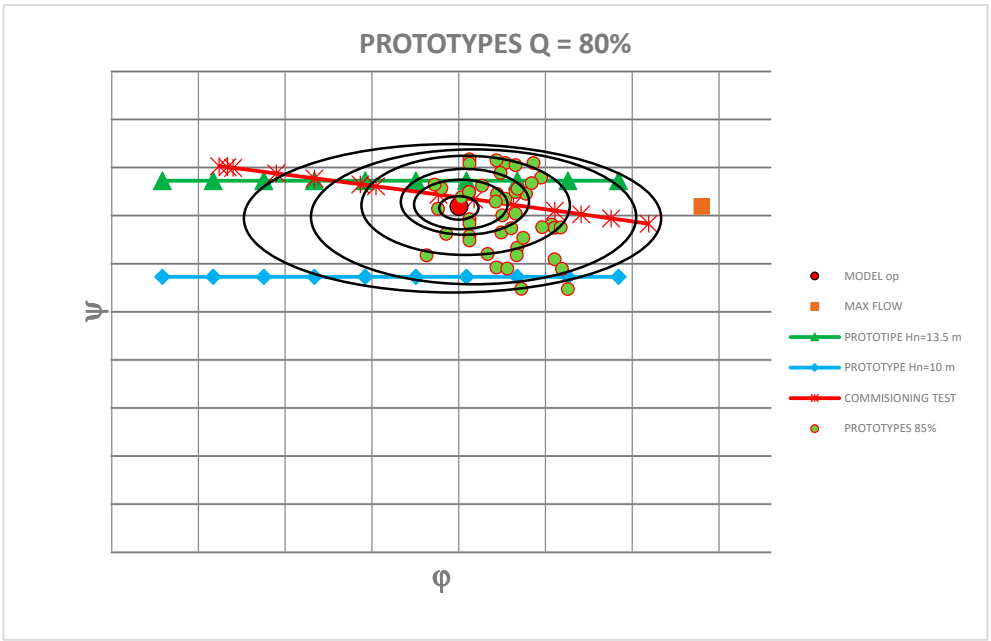

Figure 9. Working points related to the reduced flow rate.

From the data, it is observed that the operating points "tend" to be positioned to the right of the optimal contours, while in the case of 80% of the load, these points are close to the optimal conditions of the machine. In all cases, however, the maximum values never exceed those of the reference model (φ_{max}). The "strings" corresponding to the defined working points of each turbine used were inserted in the graphical construction. Each plant's efficiency values corresponding to the operational points considered and their subsequent re-elaboration were analyzed. By inserting the values on the diagram and collecting the iso-efficiency values, the contours referred to in the starting model were thus

obtained. The results (Figures 10 and 11) represent the areas of iso-efficiency referred to in the model.

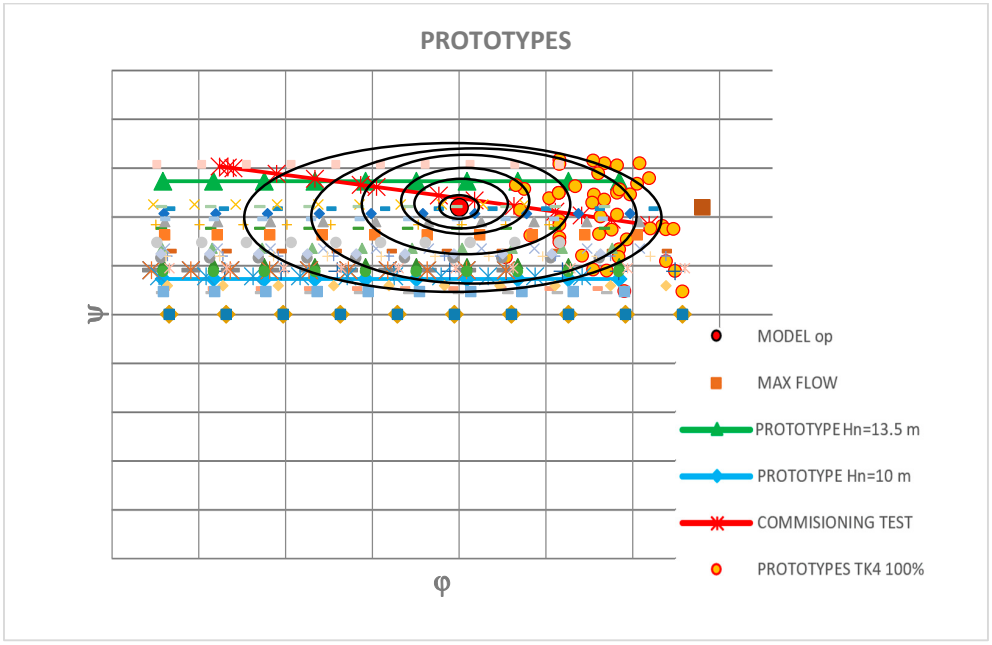

Figure 10. Iso-efficiency curve prototypes. Comparison between the prototypes (with different working heads) and the model.

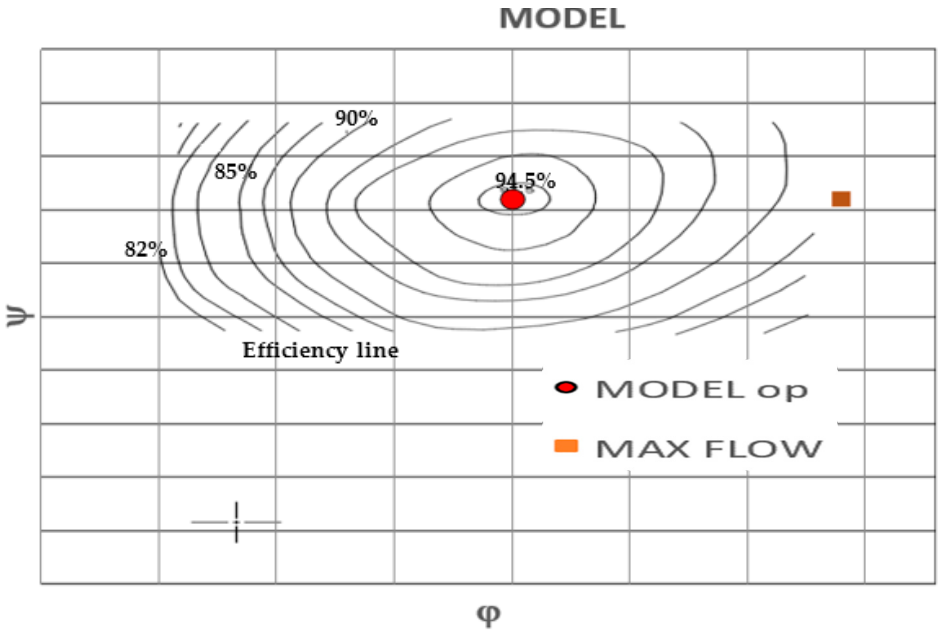

Figure 11. Iso-efficiency curve model.

4. Stator/Rotor Setup

The Kaplan turbine's birth derives from the Francis turbines' limitations at the partial flow rates [1–4,6–8,13–17]. This rapid decrease in efficiency outside the optimal range results from the progressive deformation of the velocity triangles at partial load accompanied by an increasing impact action at the inlet and a very turbulent discharge at the outlet as the V_{2t} component increases.

This circumstance could be avoided if the impellers deformed in such a way, at any load conditions, to comply with the ideal operating conditions. Hence, the idea is to

vary the angle of the impeller blades. Initially, there was the possibility of "operating" on several wheels with different angles depending on the degree of "partialization" of the vending machine. The actual "setup" (choice of the best combination between distributor opening and impeller) was a practical consequence of the first practical optimizations and the complete development of the hill charts. These concepts have been defined by Buchi (Figure 12) as follows: "We imagine having more propeller wheels with different angles β of the available blades, and we try to represent on as many contours the behavior of all these wheels, with constant head and constant rotational speed, by partializing the opening of the distributor for each case. In this way, characteristic diagrams are obtained that represent, for each "elementary" wheel, the working condition and its degree of efficiency as a function of the flow rate".

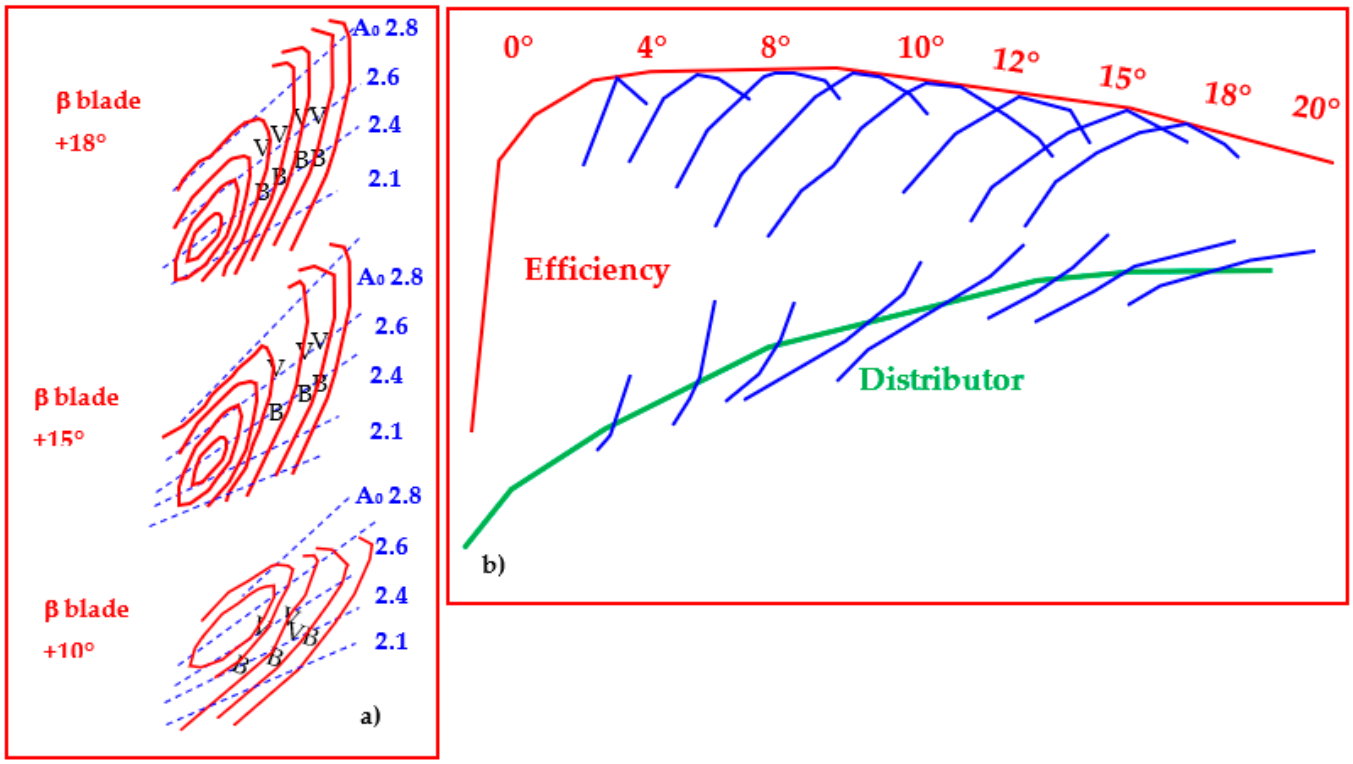

Figure 12. (**a**) Blade angle efficiency as function of distributor setup and (**b**) blade and distributor efficiency as function of blade angle.

The contour map's overlapping represents a set of iso-efficiency zones that can be collected across more significant areas of equal efficiency, as shown in Figure 13.

Therefore, an efficiency contour was obtained by replacing the impellers with different angles with a Kaplan turbine with a varying blade angle β, with the same blade profile. This contour represents the union of the individual graphs obtained using each wheel and the set of the efficiency of the elementary propellers. This methodology was consolidated in the development of scale models that were carried out in the laboratory. The result of these tests is the preparation of efficiency contours. This is all the necessary model information, which indicates the areas of iso-efficiency at the various operating points and provides additional information such as the distributor opening (specific opening A_0) and the blade's leading angle (β).

In this consideration, the importance of the "setup" condition between the opening of the impeller blades and the distributor, depending on the boundary condition (partial flow rate) and the working point (practical hydraulic head), is evident.

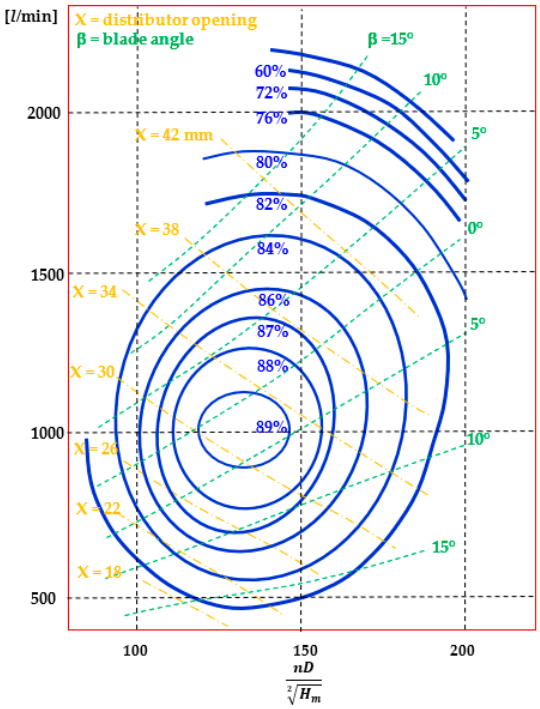

Figure 13. Typical Kaplan efficiency map.

The lack of this optimization reduces the turbine efficiency and the use of the so-called "elementary wheel", which is applied to specific operational conditions. If it is not applied precisely, it limits the "deformation" effect of the wheel, which is necessary to "center" the optimal combination. From the model efficiency contours, it is possible to identify the theoretical position of the blade angle as a function of the specific distributor opening for all working points. In the example shown (Figure 14), the coordinates for the operating point X correspond to a specific distributor opening A_0 and a blade angle β.

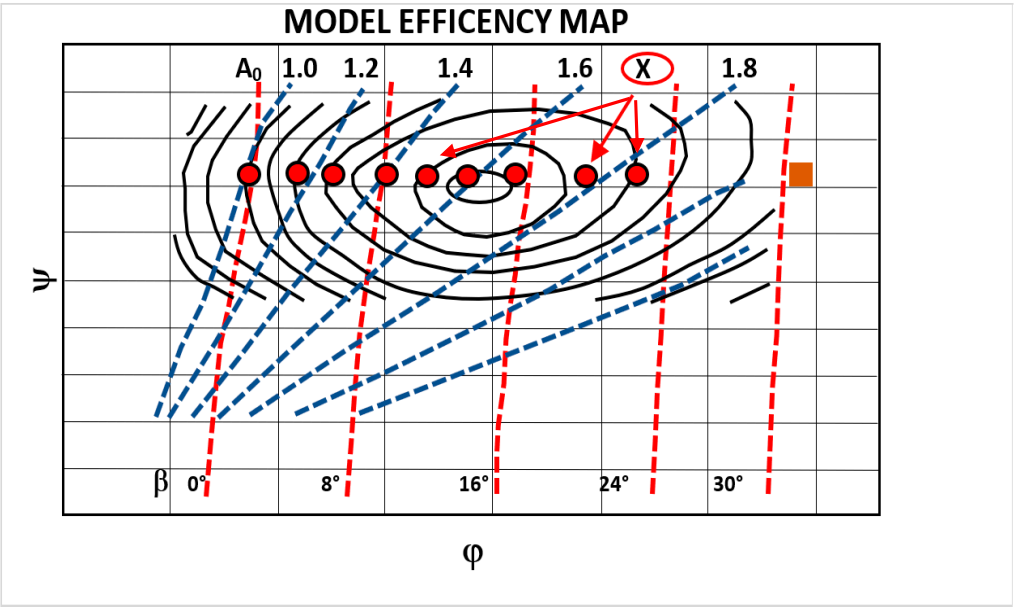

Figure 14. Efficiency map. Red dot line: β = blade angle, Blue dot line: A_0 = distributor opening, X = operating points, Brown square = max flow.

Without this information, or to better refine the calibration on the prototype, it is possible to carry out a "setup" analysis, operating with a series of practical tests. The

procedure consists of positioning the impeller blades at a particular opening β and, for this condition, varying the opening of the distributor according to specific variable values A_0. Then, for each condition, the operating parameters (flow rate, head, power) are measured and then the "elementary wheel" curve for those operating conditions is derived.

The referred value to the point of optimal efficiency corresponds to the condition of optimal setup. By processing the data relating to the test carried out, we obtained the following characteristic curves relating to the different opening conditions and each single "elementary wheel" considered (Figures 15 and 16).

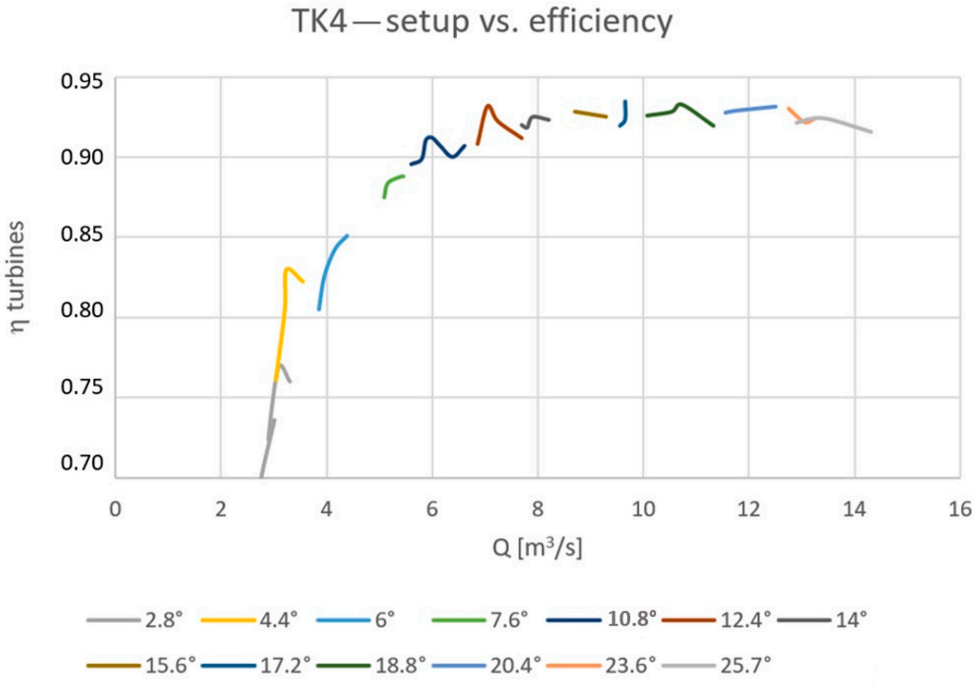

Figure 15. Model setup comparison.

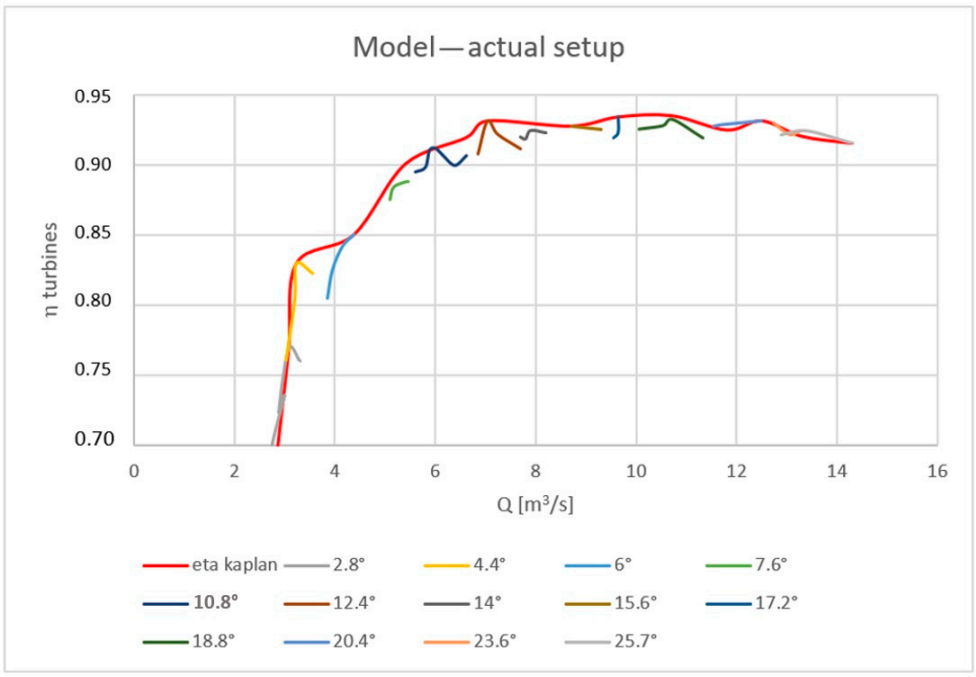

Figure 16. Optimized model setup.

By repeating the operation for the other prototypes, the coordinates relating to the blade angle and the specific opening A_0 of the distributor can be identified for each considered working point. To determine this last value, the physical dimensions (Figure 17) of the distributor (pitch diameter—passage sphere A_v) must be known to obtain the specific opening value A_0 determined as follows:

$$A_0 = \frac{A_v \cdot Z_v}{D_v}$$

where

- A_v = diameter of the passing sphere [m];
- Z_v = number of distributor blades;
- D_v = pitch diameter [m];
- A_0 = specific opening degree [m].

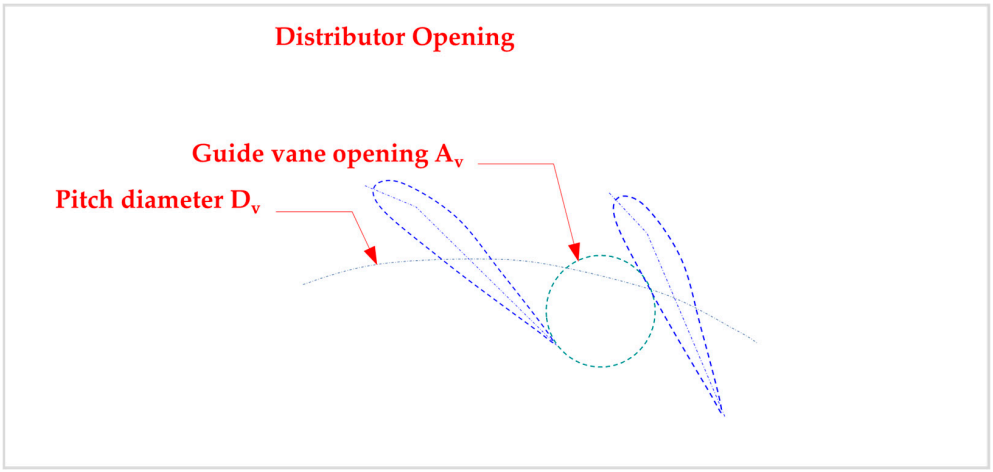

Figure 17. Setup reference scheme. The dotted blue line represents the footprint of the distributor blade.

After processing all the test data, the "points" corresponding to the various distributor opening degrees were identified, referring to parameter A_0 (Figure 18). The same criterion can be applied to the blade angle (Figure 19). Combining the three graphs provides the general diagram of the Kaplan reference model under examination (Figure 20).

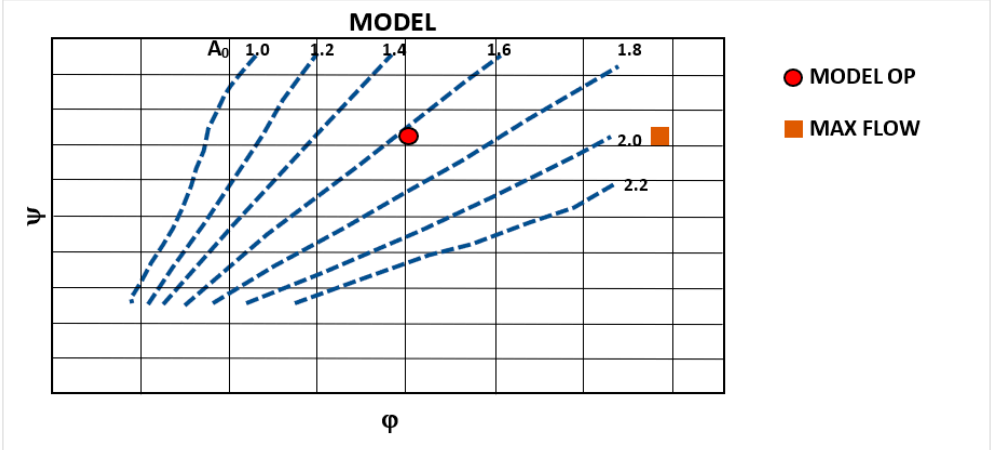

Figure 18. Determination of the operating points.

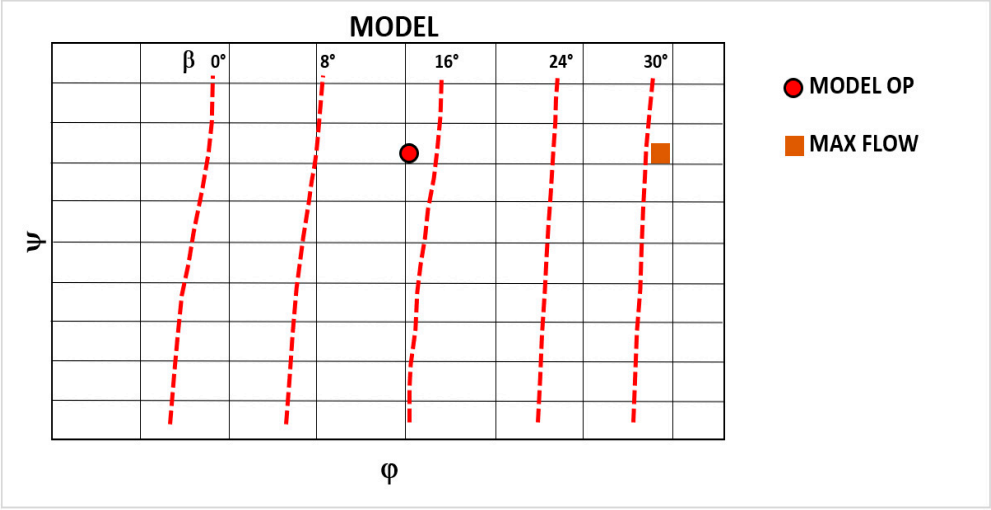

Figure 19. Operating points in the function of blade angle.

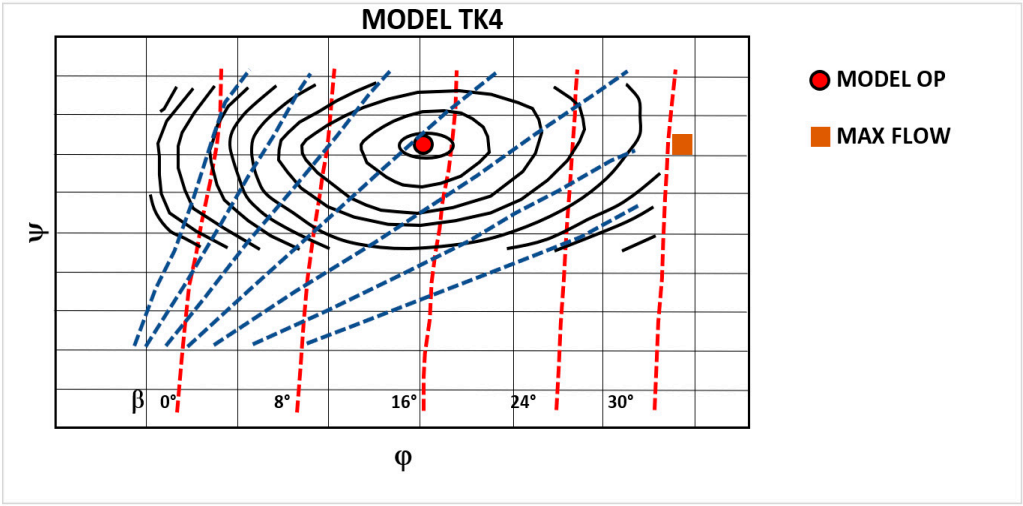

Figure 20. Operating points in the turbine map.

In addition, the nominal operating points on the diagram were plotted (Figure 21).

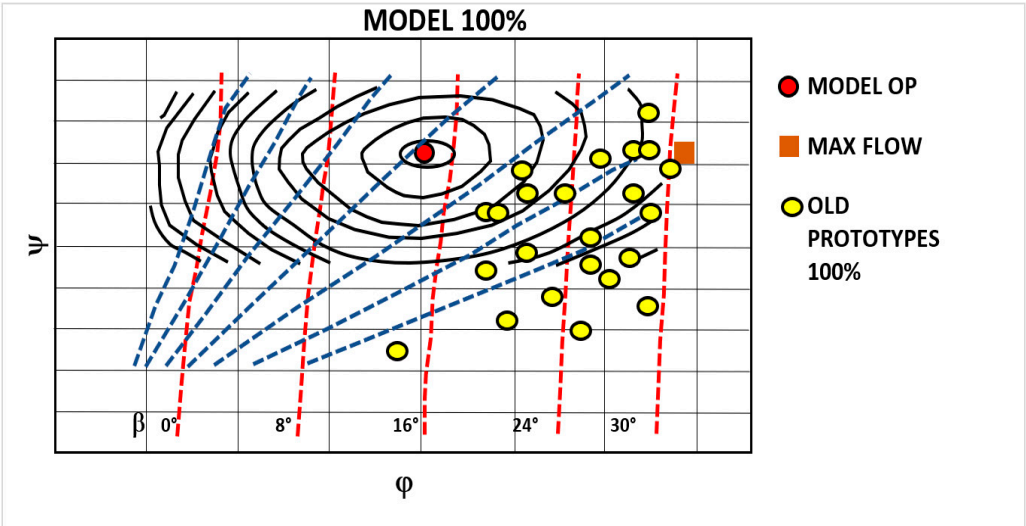

Figure 21. Kaplan turbine nominal operating points.

Finally, the behavior in 80% of the available heads was analyzed (Figure 22).

The diagram confirmed that the maximum opening condition was on the right side, and, with one exception, it fell within the maximum flow condition defined by this model. Furthermore, the optimal condition was at the center of the diagram, highlighting that the studied model had a higher centering point. This is justified because this profile has probably been studied for practical application at a generally higher head condition.

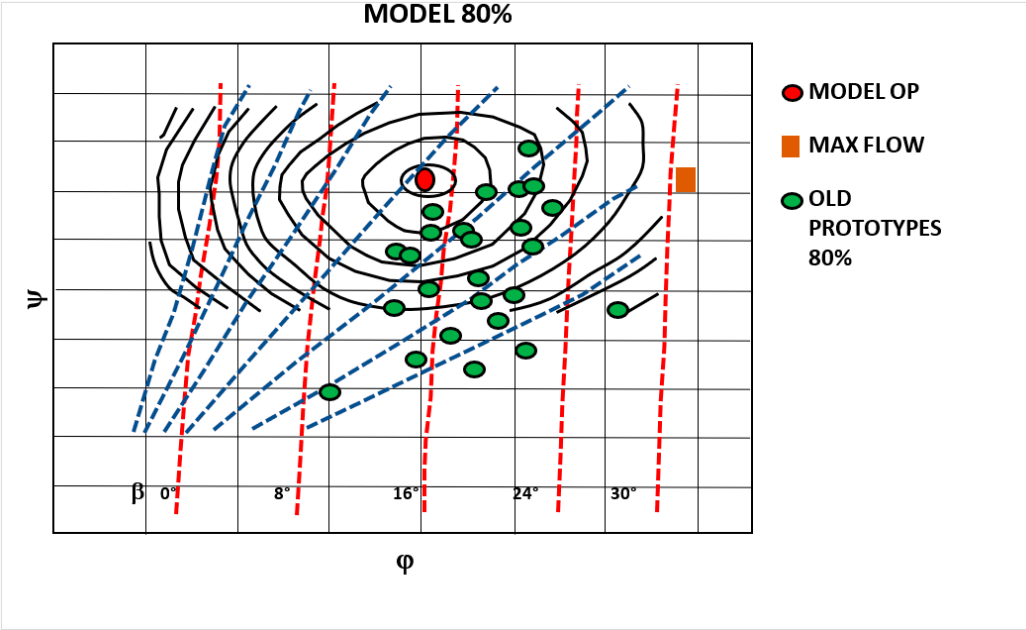

Figure 22. Turbine operating points at 80%.

5. Conclusions

This study allows the reconstruction of a contour diagram of a Kaplan turbine by analyzing the characteristic curves and field tests of machines with the same blade profile. The analysis was critical in several respects. In addition to confirming the goodness of the prototype design, which reflects very well the criteria of "centering" and maximum efficiency of the original model, it also shows the perfect correspondence of the requirements of fluid dynamic similarity between the actual prototype and the scale model. The considerable survey and mapping work also allowed, according to reverse engineering criteria [10–14], the reconstruction of the diagram of the starting contour lines of the scale model used. Although the authors do not claim the accuracy and completeness of the original turbomachinery (in fact, the analysis of the cavitation parameters is missing), the "*method presented*" provides *a handy tool* to verify the machinery application range and its behavior in case of head variation and for defining the turbine "setup". Moreover, for the various operating points, it is possible to determine the theoretical opening condition of the distributor as a function of the blade's angle.

In conclusion, the "*proposed procedure*" can be used to understand the turbine variable operational condition, especially regarding head variation. The diagrams obtained by the model allow us to visualize the performance of specific distributor openings as a function of the vertical positioning, which depends substantially on the value of the net head. Finally, the machine's so-called "overflow" conditions can be evaluated. In fact, within the limits of the right side of the diagram, identified by the condition of the model "maximum flow rate" $_{max}$, it is possible to see the available margin as a function of the trend of the maximum possible angle of the impeller blades and the specific opening of the distributor A_0.

Author Contributions: Conceptualization, R.C., A.C., G.M.B. and G.P.; methodology, R.C., A.C. and G.M.B.; software, R.C., A.C. and G.P.; validation, G.M.B.; formal analysis, R.C., G.M.B. and G.P.;

investigation, R.C., A.C., G.M.B. and G.P.; resources, R.C. and G.M.B.; data curation, R.C., A.C., G.M.B. and G.P.; writing—original draft preparation, R.C.; writing—review and editing, R.C.; visualization, R.C. and G.P.; supervision, R.C. and A.C.; project administration, R.C. and G.P. All authors have read and agreed to the published version of the manuscript.

Funding: This research received no external funding.

Data Availability Statement: Data are contained within the article.

Conflicts of Interest: The author Gian Marco Baralis is from BGM Company. The other authors declare there is no conflict of interest.

References

1. Balje, O.E. *Turbomachines: A Guide to Design, Selection and Theory*; John Wiley Sons Inc.: Hoboken, NJ, USA, 1981.
2. Dixon, S.L.; Hall, C. *Fluid Mechanics and Thermodynamics of Turbomachinery. Butterworth-Heinemann 2013*, 7th ed.; Butterworth-Heinemann: Oxford, UK, 2013.
3. Shepherd, D.G. *Principles of Turbomachinery*; MacMillan: New York, NY, USA, 1971.
4. Krivchenko, G.I. *Hydraulic Machines—Turbines and Pumps*, 2nd ed.; Lewis Publishers: Boca Raton, FL, USA; IEC: Geneva, Switzerland, 1994.
5. *IEC 60041*; Field Acceptance Tests to Determine the Hydraulic Performance of Hydraulic Turbines, Storage Pumps and Pump-Turbines. IEC: Geneva, Switzerland, 1991. Available online: https://www.saiglobal.com/pdftemp/previews/osh/iec/iec60000/60000/iec60041%7Bed3.0%7Den_d.img.pdf (accessed on 4 November 2023).
6. Vu, T.C.; Koller, M.; Gauthier, M.; Deschênes, C. Flow simulation and efficiency hill chart prediction for a Propeller turbine. In Proceedings of the 25th IAHR Symposium on Hydraulic Machinery and Systems. *IOP Conf. Ser. Earth Environ. Sci.* **2010**, *12*, 012040. [CrossRef]
7. Iliev, I.; Trivedi, C.; Dahlhaug, O.G. Simplified hydrodynamic analysis on the general shape of the hill charts of Francis turbines using shroud-streamline modeling. *Current Research in Hydraulic Turbines (CRHT) VIII. IOP J. Phys. Conf. Ser.* **2018**, *1042*, 012003. [CrossRef]
8. Guo, P.; Wang, Z.; Sun, L.; Luo, X. Characteristic analysis of the efficiency hill chart of Francis turbine for different water heads. *Adv. Mech. Eng.* **2017**, *9*, 1–8. [CrossRef]
9. *IEC 995*; Determination of the Prototype Performance from Model Acceptance Tests of Hydraulic Machines. IEC: Geneva, Switzerland, 1991.
10. *IEC 193*; Hydraulic Turbines, Storage Pumps and Pump-Turbines—Model Acceptance Tests. IEC: Geneva, Switzerland, 2019.
11. *IEC 60609*; Hydraulic Turbines, Storage Pumps and Pump-Turbines—Cavitation Pitting Evaluation—Part 1: Evaluation in Reaction Turbines, Storage Pumps and Pump-Turbines. IEC: Geneva, Switzerland, 2004.
12. *IEC 60609*; Hydraulic Turbines, Storage Pumps and Pump-Turbines—Cavitation Pitting Evaluation—Part 2: Evaluation in Pelton Turbines. IEC: Geneva, Switzerland, 2004.
13. Simão, M.; Ramos, H.M. Micro Axial Turbine Hill Charts: Affinity Laws, Experiments and CFD Simulations for Different Diameters. *Energies* **2019**, *12*, 2908. [CrossRef]
14. Borghetti, A.; Di Silvestro, M.; Naldi, G.; Paolone, M.; Alberti, M. Maximum Efficiency Point Tracking for Adjustable-Speed Small Hydro Power Plant. In Proceedings of the 16th PSCC, Glasgow, Scotland, 14–18 July 2008.
15. Cinquepalmi, F.; Piras, G. Earth Observation Technologies for Mitigating Urban Climate Changes. In *Technological Imagination in the Green and Digital Transition*; CONF.ITECH 2022. The Urban Book Series; Springer: Cham, Switzerland, 2023. [CrossRef]
16. Capata, R.; Piras, G. Condenser Design for On-Board ORC Recovery System. *Appl. Sci.* **2021**, *11*, 6356. [CrossRef]
17. Piras, G.; Muzi, F. Energy Transition: Semi-Automatic BIM Tool Approach for Elevating Sustainability in the Maputo Natural History Museum. *Energies* **2024**, *17*, 775. [CrossRef]